Sampling distributions of random electromagnetic fields in mesoscopic or dynamical systems

Luk R. Arnaut

Time, Quantum and Electromagnetics Division, National Physical Laboratory, Teddington, TW11 0LW United Kingdom
and Department of Electrical and Electronic Engineering, Imperial College of Science, Technology and Medicine,
South Kensington Campus, London, SW7 2AZ United Kingdom

We derive the sampling probability density function (pdf) of an ideal localized random electromagnetic field, its amplitude, and intensity in an electromagnetic environment that is quasistatically time-varying statistically homogeneous or static statistically inhomogeneous. The results allow for the estimation of field statistics and confidence intervals when a single spatial or temporal stochastic process produces randomization of the field. Sampling distributions are particularly significant when the number of degrees of freedom ν is relatively small (typically, $\nu < 40$), e.g., in mesoscopic systems when the sample set size N is relatively small by choice or by force. Results for both coherent and incoherent detection methods are derived for Cartesian, planar, and full-vectorial fields. We show that the functional form of the sampling pdf depends on whether the random variable is dimensioned (e.g., the sampled electric field proper) or is expressed in dimensionless standardized or normalized form (e.g., the sampled electric field divided by its sample standard deviation or sample mean). For dimensioned quantities, the electric field, its amplitude, and intensity exhibit different types of Bessel K sampling pdfs, which differ significantly from the asymptotic Gauss normal and $\chi^{(2)}_{2p}$ ensemble pdfs when ν is relatively small. By contrast, for the corresponding standardized quantities, Student t, Fisher-Snedecor F, and root-F sampling pdfs are obtained that exhibit heavier tails than comparable Bessel K pdfs. Statistical uncertainties obtained from classical small-sample theory for dimensionless quantities are shown to be overestimated compared to dimensioned quantities. Differences in the sampling pdfs arising from denormalization versus destandardization are identified.

I. INTRODUCTION

In the application of statistical methods to disordered and chaotic systems, particularly nonergodic and/or mesoscopic systems [1–6], the role played by sampling distributions [7] is of fundamental importance because, in practice, data sets are necessarily of limited (and often small) size N. Strictly, the central limit theorem (CLT) is inapplicable to finite sample sets, *a fortiori* to small sets. Therefore, sampling distributions, rather than their underlying (parent) ensemble distributions, should always be used in any proper comparison between theoretical and empirical probability distributions based on numerical data from practical measurement (experiment) or simulation (computation), particularly when detecting or validating unexpected phenomena. The finiteness of the number of degrees of freedom for sample sets, ν, can have a profound effect not only on the statistical moments, but also on the functional form and shape of the probability density function (pdf)—particularly near its extremities—and on second- or higher-order statistics, such as auto- or cross-correlation functions and associated spectral densities, etc. As a matter of fact, sampling pdfs draw on properties of both first- and second-order ensemble statistics: while the sampling distributions are representations for local instantaneous sampled fields, the value of ν as a sampling distribution parameter is governed by the correlation distance between points. This dependence on nonlocal properties of the field applies to any physically limited realizable sampled region. For sample sets in which all N values are statistically independent (as we shall further assume), $\nu = N - 1$.

Ensemble pdfs for ideal random three-dimensional (3D) electromagnetic (EM) fields are well known and have been amply investigated in various physical applications, whether in unbounded space [8] or in the presence of an impedance boundary [9]. By contrast, their associated sampling pdfs have received little attention yet are pertinent and require characterization. Idealized random (stochastic) classical EM fields offer a paradigm for characterizing wave propagation or transport governed by dynamic multiple scattering (time-varying configuration or boundaries). Examples include fields inside acoustic or EM mode-tuned or mode-stirred reverberation chambers (MT/MSRCs) [8–12], mesoscopic structures, random or turbulent media, polarization and anisotropy in, e.g., the cosmic microwave background radiation [13–15], static or dynamic optical diffusion using random-phase screens, diffusing wave spectroscopy [16–21], etc.

For the estimation of statistics of the field, amplitude, intensity, energy density, and power for such "wave chaos," the ensemble pdf of the field is usually adequate when the number of statistically independent partial contributions and, hence, ν approaches infinity. For example, for MT/MSRCs, the prerequisites are that the wavelength is very short relative to the physical dimensions of the cavity and that the observation time is long compared to the correlation time of the stirring process because, physically, a random EM field is governed by the spatial or temporal extent of the space- or time-limited process. On occasion, however, ν is too small for these ensemble pdfs to be sufficiently accurate. In this case, the CLT or maximum-entropy principle may not be applicable. Nevertheless, in such low-dimensional cases, spatial and/or temporal averaging increase the value of ν [22], which may have a substantial effect on the measured or perceived distribution of the field.

A key issue addressed in this paper is that statistically homogeneous random fields are characterized by pdfs with distribution parameters (e.g., average, standard deviation, number of degrees of freedom, etc.) whose values have to be *estimated* from the *same* set of data of the fluctuating field. As a result, these parameters themselves show sampling fluctuations because of the finite value of ν. These variations give rise to bi- or multivariate fluctuations and increased uncertainty (i.e., wider confidence intervals) for the sampled field compared to the corresponding ensemble distribution where these parameters are known exactly.

The physical origin of the limitation of the value of ν can be twofold. First, the potential (i.e., maximum attainable) number of *statistically independent* realizations, N_{max}, may be practically restricted even if an unlimited number of different states of the statistical ensemble were physically realized. For example, in a MT/MSRC, this case corresponds to the so-called undermoded regime (i.e., multimode operation but with less than, say, ten cavity modes being excited simultaneously)—typically occurring at wavelengths where modal overlap is relatively small. As another example, in a relatively small sample of a random medium, the limitation on the value of ν refers to the case of a relatively small loading fraction of inclusions. In this case, even the ensemble distribution does not possess Gauss normal statistics. Second, N_{max} may be unlimited but, for economical or other reasons, the sample size may need to be severely restricted ($N \ll N_{max}$). In this case, while ν_{max} is potentially large, the value of ν actually realized in a sample set is relatively small.

In this paper, we investigate sampling pdfs of the complex value, amplitude, and intensity of one-dimensional (1D), two-dimensional (2D), and 3D random EM fields that have ideal Gaussian ensemble probability distributions for both the actual (nonstandardized) observed EM quantities and for their standardized forms. Here, the notions of standardized and normalized random variables refer to a random quantity divided by its own (sample or ensemble) standard deviation or mean value, respectively. Coherent as well as incoherent detection methods are considered in each case. However, specific nonstationary effects associated with the dynamics of multiple scattering, which are relevant to certain aspects of diffusing wave spectroscopy [17,18], are not addressed here: each realized state of the system is considered in its quasistationary approximation. The scenario investigated here is also relevant, in particular, to several practical applications in wireless communications (e.g., mobile-to-fixed and mobile-to-mobile transmissions), signal processing, wave propagation in turbulent media, modal noise in optical fibers under restricted-mode launch conditions [20], etc.

II. ANALYTIC ELECTRIC OR MAGNETIC FIELD

A. Coherent detection

1. Nonstandardized field

Consider an analytic modulated local field $E = E' - jE''$ received by an antenna (sensor) or scatterer immersed in a time-varying multiscattering environment. A harmonic time dependence $\exp(j\omega t)$ of the carrier wave is assumed and suppressed. If this field is composed of an arbitrarily large (theoretically infinite) number of fluctuating partial fields (e.g., modal or angular plane-wave spectral components) whose realization forms a sample random walk in the complex plane [23], then, on account of the CLT (valid under very general but specific conditions [24]), the associated conditional pdf of $E'^{(\prime)}$ coincides with the ensemble pdf given by

$$f_{E'^{(\prime)}|(S_{E'^{(\prime)}}, M_{E'^{(\prime)}})}[e'^{(\prime)}|(s_{E'^{(\prime)}}, m_{E'^{(\prime)}})]$$

$$= \frac{\exp\left[-\dfrac{(e'^{(\prime)} - m_{E'^{(\prime)}})^2}{2s_{E'^{(\prime)}}^2}\right]}{\sqrt{2\pi}s_{E'^{(\prime)}}}. \qquad (1)$$

Here, $M_{E'^{(\prime)}}$ and $S_{E'^{(\prime)}}$ represent random variables induced by the sample mean and sample standard deviation of $E'^{(\prime)}$, respectively, whereas lowercase symbols $m_{E'^{(\prime)}}$ and $s_{E'^{(\prime)}}$ represent their corresponding sample values. If the mean and standard deviation of $E'^{(\prime)}$ are known with certainty, with respective constant ensemble values $\mu_{E'^{(\prime)}}$ and $\sigma_{E'^{(\prime)}}$, i.e., if

$$f_{M_{E'^{(\prime)}}}(m_{E'^{(\prime)}}) = \delta(m_{E'^{(\prime)}} - \mu_{E'^{(\prime)}}), \qquad (2)$$

$$f_{S_{E'^{(\prime)}}}(s_{E'^{(\prime)}}) = \delta(s_{E'^{(\prime)}} - \sigma_{E'^{(\prime)}}), \qquad (3)$$

then the conditional pdf (1) coincides with the marginal pdf $f_{E'^{(\prime)}}(e'^{(\prime)})$ because, in general,

$$f_{E'^{(\prime)}}(e'^{(\prime)}) = \int_{-\infty}^{+\infty} dm_{E'^{(\prime)}} \int_{0}^{+\infty} ds_{E'^{(\prime)}}$$

$$\times f_{E'^{(\prime)}, S_{E'^{(\prime)}}, M_{E'^{(\prime)}}}(e'^{(\prime)}, s_{E'^{(\prime)}}, m_{E'^{(\prime)}}), \qquad (4)$$

$$= \int_{-\infty}^{+\infty} dm_{E'^{(\prime)}} \int_{0}^{+\infty} ds_{E'^{(\prime)}}$$

$$\times f_{E'^{(\prime)}|(S_{E'^{(\prime)}}, M_{E'^{(\prime)}})}[e'^{(\prime)}|(s_{E'^{(\prime)}}, m_{E'^{(\prime)}})]$$

$$\times f_{S_{E'^{(\prime)}}, M_{E'^{(\prime)}}}(s_{E'^{(\prime)}}, m_{E'^{(\prime)}}), \qquad (5)$$

and because in (and only in) the case of a Gauss normal ensemble distribution of $E'^{(\prime)}$ are the sample mean and sample standard deviation found to be independent random variables [7], i.e., in this case

$$f_{S_{E'^{(\prime)}}, M_{E'^{(\prime)}}}(s_{E'^{(\prime)}}, m_{E'^{(\prime)}}) = f_{S_{E'^{(\prime)}}}(s_{E'^{(\prime)}})f_{M_{E'^{(\prime)}}}(m_{E'^{(\prime)}}). \quad (6)$$

From Eqs. (1)–(6), we obtain

$$f_{E'^{(\prime)}}(e'^{(\prime)}) = \frac{\exp\left[-\dfrac{(e'^{(\prime)} - \mu_{E'^{(\prime)}})^2}{2\sigma_{E'^{(\prime)}}^2}\right]}{\sqrt{2\pi}\sigma_{E'^{(\prime)}}}. \qquad (7)$$

Here, $\sigma_{E'^{(\prime)}} = \sigma_E/\sqrt{2} = \sqrt{p}\sigma_{E'^{(\prime)}_\alpha} = \sqrt{p/2}\sigma_{E_\alpha}$, where $\alpha = x, y$, or z for the three Cartesian components E_α of the vector field $\mathbf{E}$ and where the value of p corresponds to the number of spatial dimensions in which $\mathbf{E}$ is being considered.

Of the possible values of p, *viz.*, 1, 2, or 3, its specific value is governed by the polarization direction of the field

sensor and/or by any EM excitation or boundary conditions that may enforce a fixed (deterministic) polarization state of the field. Thus, the Cartesian component of a vector field and the 3D vector field itself correspond to the cases $p=1$ and $p=3$, respectively. For a paraxially propagating polarized or unpolarized optical random field, $p=1$ or $p=2$, respectively. The case $p=2$ refers to an unpolarized electric field that is transverse to the local wave vector (i.e., randomly elliptically polarized field) and will be denoted by a subscript "t," whereas $p=1$ corresponds to its polarized detection or to a randomly modulated linearly polarized field, denoted by a subscript "α." These values of p apply to local fields detected by an electrically small sensor, whose characteristic length is less than the spatial coherence length of the field, i.e., less than typically $\lambda/2$ in an unbounded medium. Larger values of p apply to electrically large detectors whose receiving cross section (whether physical or as a synthetic aperture) is larger than $\lambda/2$ in one or more dimensions. For example, for currents induced in a wire antenna of length L, we have $p=\max[1, L/(\lambda/2)]$.

If, instead of Eq. (3), $S_{E'^{(\prime)}}$ exhibits random fluctuations or if its value is not known precisely, the sampling pdf of $S_{E'^{(\prime)}}$ for Gaussian $E'^{(\prime)}|S_{E'^{(\prime)}}$ is a χ_{pN-1} pdf, i.e.,

$$f_{S_{E'^{(\prime)}}}(s_{E'^{(\prime)}};N) = \frac{C_{S_{E'^{(\prime)}}}}{\sigma_{S_{E'^{(\prime)}}}} \left(\frac{s_{E'^{(\prime)}}}{\sigma_{S_{E'^{(\prime)}}}} \right)^{pN-2} \exp\left[-\mathcal{N}\left(\frac{s_{E'^{(\prime)}}}{\sigma_{S_{E'^{(\prime)}}}} \right)^2 \right],$$

$$(8)$$

with

$$C_{S_{E'^{(\prime)}}} \triangleq \frac{2\mathcal{N}^{(pN-1)/2}}{\Gamma\left(\dfrac{pN-1}{2} \right)}, \qquad (9)$$

$$\mathcal{N} \triangleq \frac{pN-1}{2} - \left[\frac{\Gamma\left(\dfrac{pN}{2} \right)}{\Gamma\left(\dfrac{pN-1}{2} \right)} \right]^2. \qquad (10)$$

The sampling pdf (8) is expressed in its self-sufficient form [22], i.e., it contains the standard deviation of $S_{E'^{(\prime)}}$ itself as a distribution parameter. Alternatively, Eq. (8) can be re-expressed in terms of the ensemble standard deviation $\sigma_{E'^{(\prime)}}$ of $E'^{(\prime)}$ because both statistics are related via

$$\sigma_{S_{E'^{(\prime)}}} = \sigma_{E'^{(\prime)}} \sqrt{\frac{2\mathcal{N}}{pN-1}}. \qquad (11)$$

Then, with the aid of [[25], Eq. (3.471.9)], the sampling pdf of $E'^{(\prime)}$ for $\mu_{E'^{(\prime)}}=0$ in Eq. (5) is obtained as a marginal pdf of the joint sampling pdf $f_{E'^{(\prime)},S_{E'^{(\prime)}}}(e'^{(\prime)},s_{E'^{(\prime)}};N)$, viz.,

$$f_{E'^{(\prime)}}(e'^{(\prime)};N)$$

$$= \int_0^{+\infty} f_{E'^{(\prime)}|S_{E'^{(\prime)}}}(e'^{(\prime)}|s_{E'^{(\prime)}}) f_{S_{E'^{(\prime)}}}(s_{E'^{(\prime)}};N) ds_{E'^{(\prime)}}$$

$$= \frac{(pN-1)^{(pN-1)/2}}{2^{pN/2}\sqrt{\pi}\Gamma\left(\dfrac{pN-1}{2} \right)\sigma_{E'^{(\prime)}}^{pN-1}}$$

$$\times \int_0^{+\infty} t^{pN/2-2} \exp\left(-\frac{e'^{(\prime)2}}{2t} - \frac{pN-1}{2}\frac{t}{\sigma_{E'^{(\prime)}}^2} \right) dt,$$

$$(12)$$

i.e.,

$$f_{E'^{(\prime)}}(e'^{(\prime)};N)$$

$$= \frac{C_{E'^{(\prime)}}}{\sigma_{E'^{(\prime)}}} \left(\frac{|e'^{(\prime)}|}{\sigma_{E'^{(\prime)}}} \right)^{pN/2-1} K_{pN/2-1}\left(\sqrt{pN-1}\frac{|e'^{(\prime)}|}{\sigma_{E'^{(\prime)}}} \right), \qquad (13)$$

with

$$C_{E'^{(\prime)}} \triangleq \frac{(pN-1)^{pN/4}}{2^{pN/2}\sqrt{\pi}\Gamma\left(\dfrac{pN-1}{2} \right)}. \qquad (14)$$

The pdf (13) belongs to McKay's class of Bessel K distributions [26]. These distributions have also been obtained in a variety of applied statistical problems in electromagnetics and elsewhere (cf., e.g., [27], [28], and references in [23]). It is further worth noting that the pdf (13) has also been obtained in a different case, *viz.*, as an ensemble pdf associated with an *ad hoc* Bessel K distributed field amplitude (implying non-Gaussian/non-Rayleigh ensemble statistics) and derived via a Blanc-Lapierre transformation [4]. Results that are at least qualitatively compliant with those obtained from the pdf (13) have been observed recently in experiments involving correlated scattering [6]. The pdf (13) is also included in the class of Meijer G limit pdfs for complex fields in undermoded MT/MSRCs [23], which in turn is a special case of more general Fox H distributions [29].

It is emphasized that the result (13) strictly holds for a physically ideal, *viz.*, Gaussian random field if it is subjected to a finite-sized sampling (detection) process. Only in this case is a Gaussian marginal pdf $f_{E'^{(\prime)}|S_{E'^{(\prime)}}}$ compatible with a non-delta-distributed $S_{E'^{(\prime)}}$. For the physical field itself, a Gaussian $f_{E'^{(\prime)}|S_{E'^{(\prime)}}}$ implies the number of degrees of freedom approaching infinity, hence resulting in a delta distribution for $f_{S_{E'^{(\prime)}}}$ and vice versa.

Figure 1(a) shows the pdf (13) for selected values of N. Because of symmetry of $f_{E'^{(\prime)}}$ with respect to its mean value, only the positive half of the distribution is shown. The figure indicates that lowering the value of N gives rise to heavier tails and increased kurtosis of the sampling pdf (leptokurtic) compared to the Gauss normal asymptotic, i.e., ensemble pdf $(N\to+\infty)$.
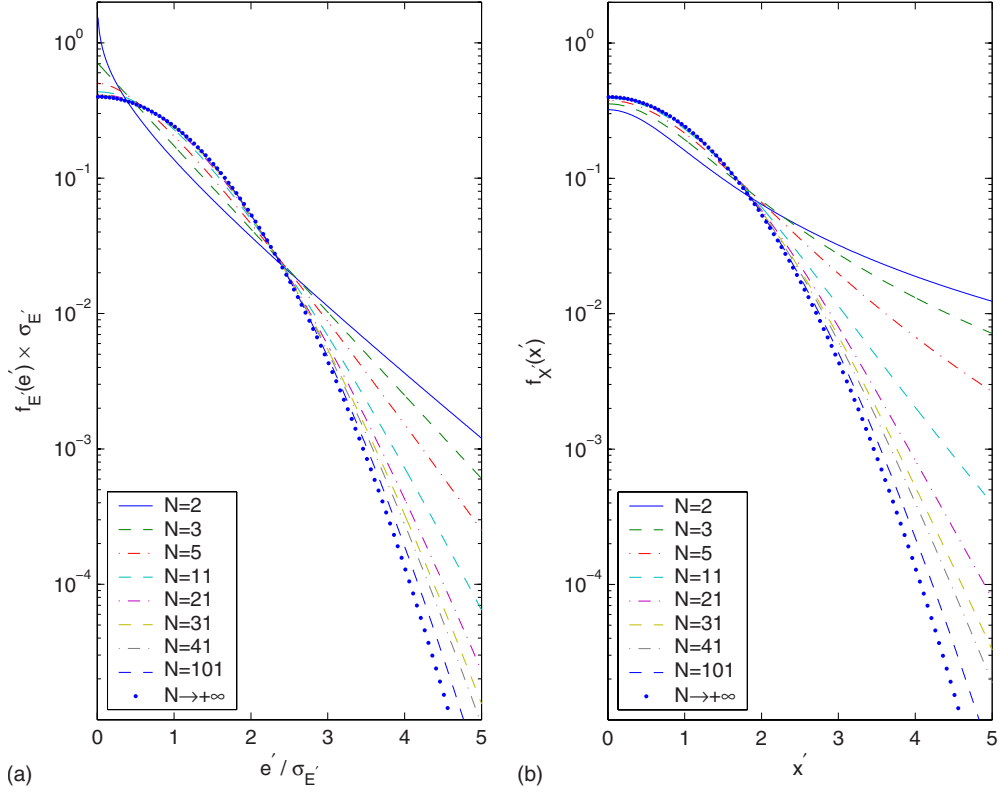
FIG. 1. (Color online) Sampling probability density function for real or imaginary Cartesian component of electric field ($p=1$) at selected values of N. (a) Bessel K sampling pdfs of $E_\alpha'^{(\prime)}$ [Eq. (13)]. (b) Student t sampling pdfs of $X'^{(\prime)} = E_\alpha'^{(\prime)}/S_{E_\alpha'^{(\prime)}}$ [Eq. (19)]. In both plots, the right tail becomes thinner for increasing values of N.

More generally, if $E'^{(\prime)}$ exhibits a deterministic, i.e., constant bias $\mu_{E'^{(\prime)}}$ as in Eq. (7), then

$$f_{E'^{(\prime)}}(e'^{(\prime)};N) = \frac{C_{E'^{(\prime)}}}{\sigma_{E'^{(\prime)}}} \left(\frac{|e'^{(\prime)} - \mu_{E'^{(\prime)}}|}{\sigma_{E'^{(\prime)}}} \right)^{pN/2-1}$$
$$\times K_{pN/2-1}\left(\sqrt{pN-1} \frac{|e'^{(\prime)} - \mu_{E'^{(\prime)}}|}{\sigma_{E'^{(\prime)}}} \right). \quad (15)$$

For non-negligible "slow" fluctuations of $m_{E'^{(\prime)}}$ in Eq. (1), i.e., for a random bias (trend) of $E'^{(\prime)}$, the results are easily generalized as follows. On account of linearity, the sampling variable $M_{E'^{(\prime)}}$ for Gaussian $E'^{(\prime)}$ is also Gaussian with the same expected value but standard deviation $\sigma_{E'^{(\prime)}}/\sqrt{N}$. Therefore, if the bias is itself random with Gauss normal distribution, i.e., if

$$f_{M_{E'^{(\prime)}}}(m_{E'^{(\prime)}};N) = \frac{\exp\left[-\dfrac{N(m_{E'^{(\prime)}} - \mu_{E'^{(\prime)}})^2}{2\sigma_{E'^{(\prime)}}^2} \right]}{\sqrt{2\pi/N}\,\sigma_{E'^{(\prime)}}} \quad (16)$$

instead of Eq. (2), then with Eqs. (5) and (6), we arrive at

$$f_{E'^{(\prime)}}(e'^{(\prime)};N) = \frac{C'_{E'^{(\prime)}}}{\sigma_{E'^{(\prime)}}} \int_{-\infty}^{+\infty} |e'^{(\prime)} - m_{E'^{(\prime)}}|^{pN/2-1}$$
$$\times \exp\left[-\frac{N(m_{E'^{(\prime)}} - \mu_{E'^{(\prime)}})^2}{2\sigma_{E'^{(\prime)}}^2} \right]$$
$$\times K_{pN/2-1}\left(\sqrt{pN-1} \frac{|e'^{(\prime)} - m_{E'^{(\prime)}}|}{\sigma_{E'^{(\prime)}}} \right) dm_{E'^{(\prime)}}.$$
$$(17)$$

For practical numerical integration of Eq. (17), the double-infinite range of $m_{E'^{(\prime)}}$ can be limited to, say, $[\mu_{E'^{(\prime)}} - 5\sigma_{E'^{(\prime)}}/\sqrt{N},\ \mu_{E'^{(\prime)}} + 5\sigma_{E'^{(\prime)}}/\sqrt{N}]$.

For sufficiently large N, the field $E'^{(\prime)}$ and its sample mean $M_{E'^{(\prime)}}$ are approximately independent (sharing $N-1$ degrees of freedom), whence $E'^{(\prime)} - M_{E'^{(\prime)}}$ is then also Gaussian with zero mean and standard deviation $\sigma_{E'^{(\prime)}}^* \simeq \sigma_{E'^{(\prime)}}\sqrt{1+1/N}$. Thus, Eq. (15) with $\sigma_{E'^{(\prime)}}$ replaced by $\sigma_{E'^{(\prime)}}^*$ serves as a first-order approximation to the pdf (17) for large N.

2. Standardized field

For comparison of an empirical distribution against a theoretical sampling distribution, it is necessary to standardize the experimental values of $E'^{(\prime)}$. Then, rather than determin-

ing the pdf of $E'^{(\prime)}$, we require the pdf of the dimensionless variate

$$X'^{(\prime)} \triangleq \frac{E'^{(\prime)} - M_{E'^{(\prime)}}}{S_{E'^{(\prime)}}}, \qquad (18)$$

i.e., for uncertain sample values of $M_{E'^{(\prime)}}$ and $S_{E'^{(\prime)}}$ that are unknown *a priori*. Their values are often to be estimated from the *same* limited sample data set of $E'^{(\prime)}$. For Gaussian $E'^{(\prime)}$, the $M_{E'^{(\prime)}}$ and $S_{E'^{(\prime)}}$ are statistically independent and their sampling distributions are Gaussian and χ_{pN-1}, respectively [30]. We further assume that the fluctuations of $M_{E'^{(\prime)}}$ are small compared to those of $S_{E'^{(\prime)}}$ and, *a fortiori*, $E'^{(\prime)}$.

It is shown in Sec. 1 of the Appendix that $X'^{(\prime)}$ for $M_{E'^{(\prime)}} = 0$ exhibits a Student t distribution [31] with $pN-1$ degrees of freedom, i.e.,

$$f_{X'^{(\prime)}}(x'^{(\prime)}; N) = C_{X'^{(\prime)}} \left(1 + \frac{x'^{(\prime)2}}{pN - 1} \right)^{-pN/2}, \qquad (19)$$

with $X'^{(\prime)} \triangleq E'^{(\prime)}/S_{E'^{(\prime)}}$ for $\langle E'^{(\prime)} \rangle = 0$, where the sample value $x'^{(\prime)} = e'^{(\prime)}/s_{E'^{(\prime)}}$ is estimated as a (dimensionless) ratio of the two sample values $e'^{(\prime)}$ and $s_{E'^{(\prime)}}$ and where

$$C_{X'^{(\prime)}} \triangleq \frac{\Gamma\left(\dfrac{pN}{2}\right)}{\Gamma\left(\dfrac{pN-1}{2}\right)\sqrt{(pN-1)\pi}}. \qquad (20)$$

The pdf (19) can be used to compare the empirical distribution of the measured standardized complex field against its ideal theoretical sampling distribution, particularly when N is relatively small ($N \sim 40$ or less). For example, for multiscattering contributions, the value of N can be associated with the number of scattering centers surrounding the receiver and/or the states during the motion of the environment around a momentarily stationary receiver.

Without loss of generality, we further consider a deterministically unbiased field ($\mu_{E'^{(\prime)}} = 0$). Figure 1(b) shows the pdf of $X'^{(\prime)}$ for selected values of N. Again, only the positive half of the distribution is shown. It can be seen that, compared to the asymptotic Gauss normal pdf, differences with $f_{E'^{(\prime)}}$ in Fig. 1(a) occur mainly near the origin and in the tails: the sampling pdfs are now platykurtic and their tails are even heavier.

B. Incoherent detection

Of significant practical importance, particular for measurements at optical wavelengths, is the case where the random field is sampled incoherently, i.e., by square-law detection of the electric or magnetic power, energy, or intensity devoid of phase information. Yet one may wish to extract an estimated sampling pdf for the in-phase or quadrature electric or magnetic field from such a scalar measurement. To this end, we borrow results derived in Sec. III A and restrict further analysis to the case of a circular $f_E(e)$. [For an elliptic $f_E(e)$, data for a second linearly independent quadratic form of E' and E'' are needed, e.g., $E'^2 - E''^2$.] From the derivation in Sec. III A, it follows that the sampling pdf of

$U'^{(\prime)} \triangleq E'^{(\prime)2}$ is Eq. (26) with p replaced by $p/2$ because the ensemble pdf of $U'^{(\prime)}|S_{U'^{(\prime)}}$ is χ_p^2 whereas $f_{U'^{(\prime)}}$ has a χ_{pN-1}^2 sampling pdf. With the variate transformation $f_{E'^{(\prime)}}(e'^{(\prime)}) = 2|e'^{(\prime)}| f_{U'^{(\prime)}}(u'^{(\prime)} = e'^{(\prime)2})$, we arrive at

$$f_{E'^{(\prime)}}(e'^{(\prime)}; N) = C''_{E'^{(\prime)}} \left(\frac{|e'^{(\prime)}|}{\sqrt{\sigma_U}} \right)^{[p(N+1)-3]/2}$$

$$\times K_{[p(N-1)-1]/2}\left(\sqrt{\sqrt{2p}(pN-1)} \frac{|e'^{(\prime)}|}{\sqrt{\sigma_U}} \right). \qquad (21)$$

For detection of a Cartesian component of intensity or power, i.e., $p = 1$, Eq. (21) is equivalent with Eq. (13).

III. FIELD INTENSITY (ENERGY DENSITY, POWER)

For the field intensity $U = U' + U'' = |E|^2$—as well as for the energy density or power, which are proportional to U—we can determine its sampling pdf either on the basis of measured in-phase and/or quadrature components of the field (i.e., coherent detection, e.g., using a vector network analyzer) or measured directly using a square-law detector (i.e., incoherent detection, e.g., using a power meter, spectrum analyzer, field probe, etc.). We determine sampling pdfs for both cases.

A. Incoherent detection

1. Nonstandardized intensity

In many practical cases, the intensity or energy density is measured or perceived through a square-law detector or perception process. Compared to $f_{E'^{(\prime)}|S_{E'^{(\prime)}}}$ for coherent detection, the pertinent conditional pdf (cpdf) is now $f_{U|S_U}$. On account of the CLT, the sampling cpdf for $U|S_U$ is χ_{2p}^2, i.e.,

$$f_{U|S_U}(u|s_U) = \frac{p^{p/2}}{\Gamma(p)s_U}\left(\frac{u}{s_U}\right)^{p-1}\exp\left(-\sqrt{p}\,\frac{u}{s_U}\right). \qquad (22)$$

The sampling pdf of S_U, associated with an underlying circular Gauss normal E, is a χ_{2pN-1}^2 pdf, i.e.,

$$f_{S_U}(s_U; N) = \frac{\left(pN - \dfrac{1}{2}\right)^{(pN-1/2)/2}}{\Gamma\left(pN - \dfrac{1}{2}\right)\sigma_{S_U}}\left(\frac{s_U}{\sigma_{S_U}}\right)^{pN-3/2}$$

$$\times \exp\left(-\sqrt{pN - \frac{1}{2}}\,\frac{s_U}{\sigma_{S_U}}\right), \qquad (23)$$

with

$$\sigma_{S_U} = \frac{\sigma_U}{\sqrt{pN - \dfrac{1}{2}}}. \qquad (24)$$

Performing a similar calculation as in Sec. II A 1 and again using [[25], Eq. (3.471.9)] yields the sampling pdf of U as a marginal pdf of $f_{U,S_U}(u, s_U; N)$. A Bessel K distribution is
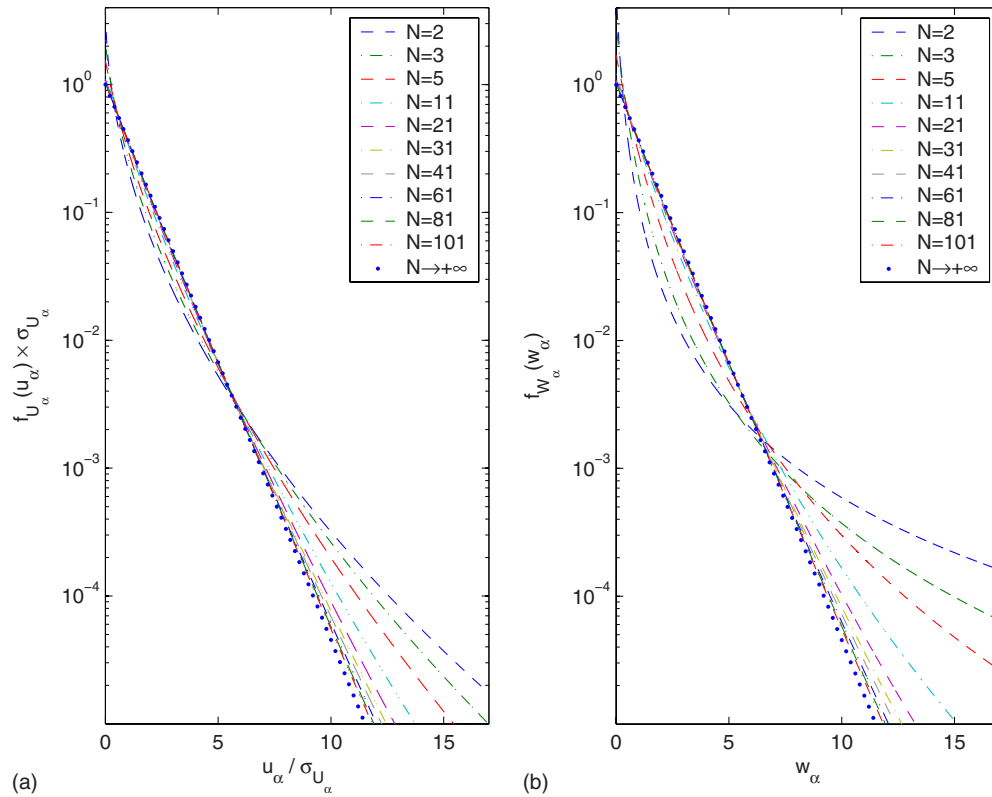
FIG. 2. (Color online) Sampling probability density function for intensity or energy density of Cartesian component of field ($p=1$) at selected values of N based on incoherent detection. (a) Bessel K sampling pdfs of U_α [Eq. (26)]. (b) Fisher-Snedecor F sampling pdfs of $W_\alpha = U_\alpha / S_{U_\alpha}$ [Eq. (29)]. In both plots, the right tail becomes thinner for increasing values of N.

again obtained, but compared to Eq. (13), it is now of a different type (i.e., the exponent of the power and the order of the Bessel function differ by a different amount), *viz.*,

$$f_U(u;N) = \int_0^{+\infty} f_{U|S_U}(u|s_U) f_{S_U}(s_u;N) ds_U$$

$$= \frac{C_U}{\sigma_U} \left(\frac{u}{\sigma_U} \right)^{[p(N+1)-5/2]/2} \quad (25)$$

$$\times K_{p(N-1)-1/2} \left(2 \sqrt{\sqrt{p} \left(pN - \frac{1}{2} \right)} \sqrt{\frac{u}{\sigma_U}} \right), \quad (26)$$

with normalization constant C_U given by

$$C_U \triangleq \frac{2}{\Gamma(p) \Gamma \left(pN - \frac{1}{2} \right)} p^{[p(N+1)-1/2]/4}$$

$$\times \left(pN - \frac{1}{2} \right)^{[p(N+1)-1/2]/2}. \quad (27)$$

It is remarkable that for the case $p=1$, the same type of Bessel K distribution (26) has been obtained in the context of sea echo for microwave radar [2], but as an *ensemble* pdf of U_α based on different starting assumptions, *viz.*, for a finite random walk in the complex plane that assumes a randomly fluctuating and large but finite number of steps (independent scattering contributions) that is distributed according to a

negative binomial distribution, as a discretization of a gamma distribution for continuous stepping. For general values of p, the pdf (26) was also obtained in [23] as a limit distribution for imperfect reverberation based on a Bayesian model for a physical process of omnidirectional scattering. Hence, the present derivation of Eq. (26) shows that Bessel K distributions are far more universal than previously thought, as they can arise under the much less restrictive condition of a mere small-sample effect for an underlying Gaussian field, as opposed to a need for any functional form of *a priori* distributions for a fluctuating ν, whether chosen *ad hoc* or otherwise. As shown in this paper, any apparent departure of an empirical field distribution from an underlying Gauss normal field distribution must be interpreted with due care and does not necessarily point to physical nonlinearity. The identification of Bessel K distributions as sampling distributions for small sample sets of received power is supported by measurements of the evolution of the distribution function of pulsed energy in a reverberant cavity [32]. Such evolution is characterized by a steady growth in the number of multipath components and, hence, ν.

Figures 2(a), 3(a), and 4(a) show the pdf (26) of incoherently detected Cartesian ($p=1$), planar ($p=2$), and total ($p=3$) field intensities, respectively, for selected values of N. The heavier tail and the sharper peak at the mode of the distribution for smaller values of N are characteristic features. Figure 5(a) shows the standardized standard deviation of Eq. (26) for these three cases as a function of N.
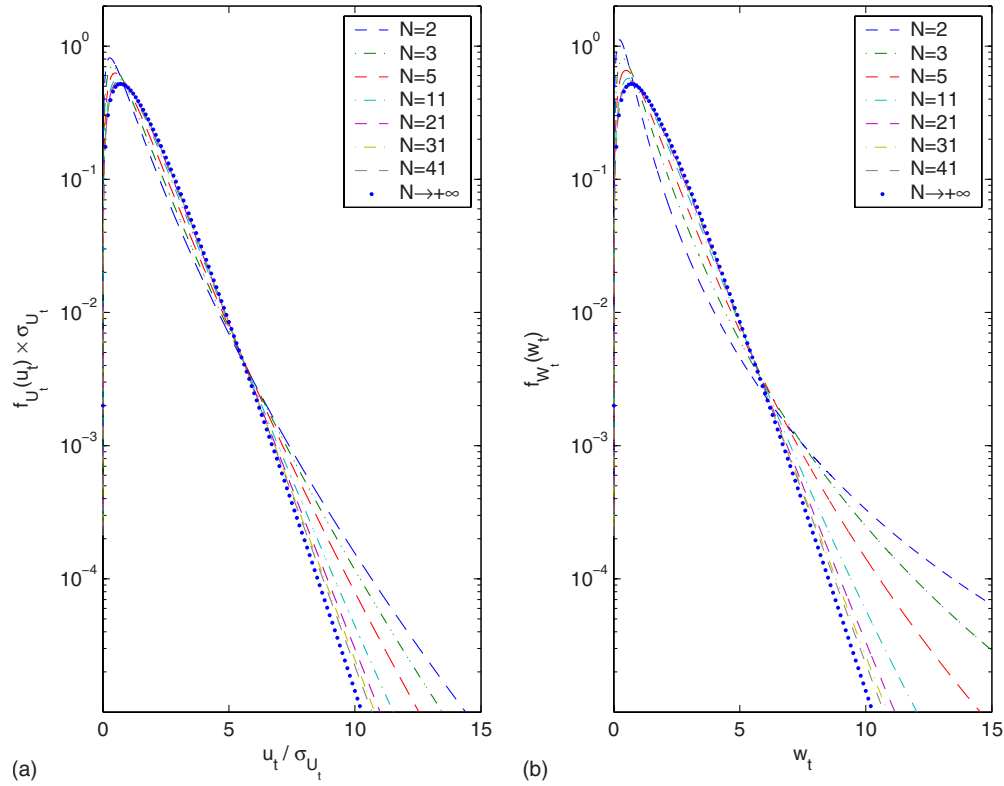
FIG. 3. (Color online) Probability density function of intensity or energy density of planar field ($p=2$) at selected values of N based on incoherent detection. (a) Bessel K sampling pdfs of U_t [Eq. (26)]. (b) Fisher-Snedecor F sampling pdfs of $W_t=U_t/S_{U_t}$ [Eq. (29)]. In both plots, the right tail becomes thinner for increasing values of N.

2. Standardized intensity

For comparison to the empirical pdf, we consider the sampling pdf of the ratio of the random variables U and S_U, viz.,

$$W \triangleq \frac{U}{S_U}. \qquad (28)$$

The calculation of $f_W(w;N)$ is detailed in Sec. 2 of the Appendix. The result is a Fisher-Snedecor F distribution

$$f_W(w;N) = C_W\, w^{p-1}\left(1 + \frac{\sqrt{p}}{pN-\frac{1}{2}}w\right)^{-[p(N+1)-1/2]}, \qquad (29)$$

as a counterpart of Eq. (19), where

$$C_W \triangleq \frac{p^{p/2}}{\left(pN-\frac{1}{2}\right)^p}\frac{\Gamma\!\left(pN-\frac{1}{2}+p\right)}{\Gamma\!\left(pN-\frac{1}{2}\right)\Gamma(p)}. \qquad (30)$$

The pdfs (29) for the incoherently detected and sample-standardized Cartesian ($p=1$), planar ($p=2$), and total ($p=3$) field intensities W_α, W_t, and W are shown in Figs. 2(b), 3(b), and 4(b), respectively, at selected values of N. Comparison between the K distributed intensities with their F distributed sample-standardized values in Figs. 2–4 shows that, for a given value of N, the sampling pdf of W exhibits a more pronounced spread than for U, owing to the larger un-

certainty of W caused by fluctuations of S_U. Figure 5(b) shows the standardized standard deviation of Eq. (29) for the three cases, indicating much larger values for small N compared to those in Fig. 5(a) for nonstandardized intensities.

3. Nonstandardized vs. non-normalized intensity

In Sec. III A 1, $f_U(u;N)$ was obtained via the sample-*standardized* variate U/S_U in the cpdf (22). However, since $\mu_U \neq 0$, we could have equally used the sample-*normalized* variate U/M_U for the cpdf to reference the data in this case. To this end, instead of Eq. (25), we now use

$$f_U(u;N) = \int_0^{+\infty} f_{U|M_U}(u|m_U) f_{M_U}(m_u;N)\,dm_U, \qquad (31)$$

with [30]

$$f_{U|M_U}(u|m_U) = \frac{p^p}{\Gamma(p)m_U}\left(\frac{u}{m_U}\right)^{p-1}\exp\!\left(-p\frac{u}{m_U}\right), \qquad (32)$$

$$f_{M_U}(m_U;N) = \frac{(pN)^{pN/2-1}}{\Gamma(pN)\sigma_{M_U}}\left(\frac{m_U}{\sigma_{M_U}}\right)^{pN-1}\exp\!\left(-\sqrt{pN}\frac{m_U}{\sigma_{M_U}}\right), \qquad (33)$$

and $\mu_U = m_U$, $\sigma_U = \sqrt{N}\sigma_{M_U}$, whence Eq. (31) becomes
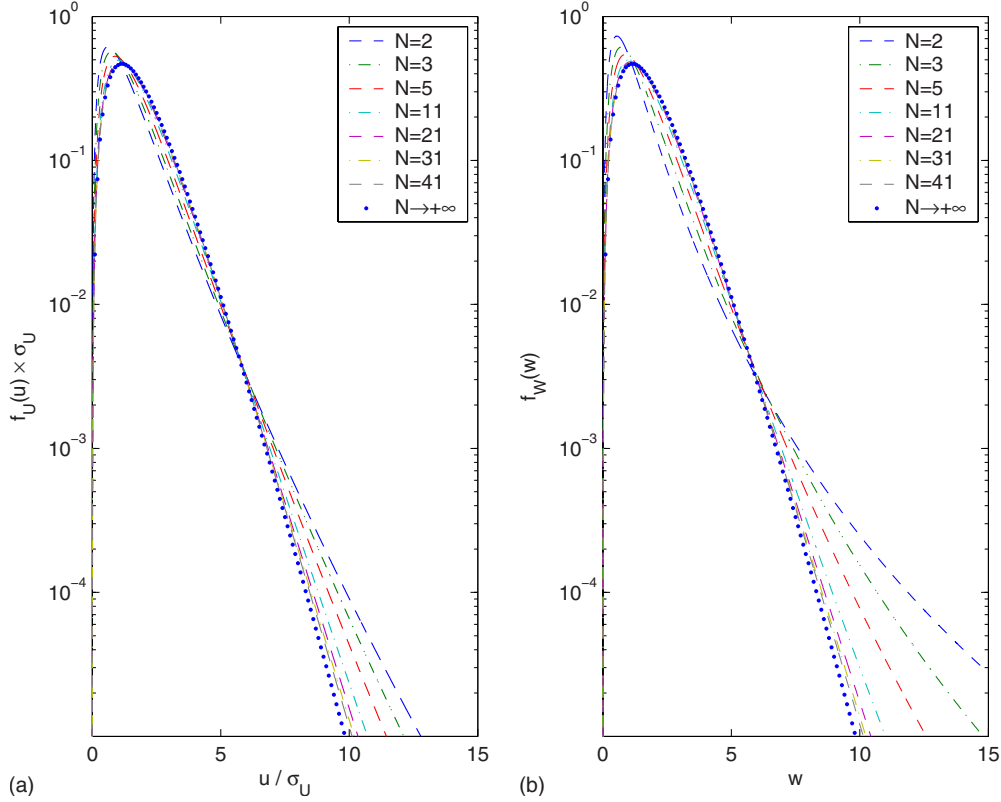
FIG. 4. (Color online) Probability density function of intensity or energy density of total (vector) field ($p=3$) at selected values of N based on incoherent detection. (a) Bessel K sampling pdfs of U [Eq. (26)]. (b) Fisher-Snedecor F sampling pdfs of $W=U/S_U$ [Eq. (29)]. In both plots, the right tail becomes thinner for increasing values of N.

$$f_U(u;N) = \frac{C_U'}{\sigma_U}\left(\frac{u}{\sigma_U}\right)^{p(N+1)/2-1}$$

$$\times K_{p(N-1)}\left(2p^{3/4}\sqrt{N}\sqrt{\frac{u}{\sigma_U}}\right), \qquad (34)$$

with normalization constant C_U' given by

$$C_U' \triangleq \frac{2p^{3p(N+1)/4}N^{p(N+1)/2}}{\Gamma(p)\Gamma(pN)}. \qquad (35)$$

The form (34) is readily re-expressed in terms of μ_U by replacing σ_U with $\mu_U/\sqrt{p}$. Comparing Eqs. (34) and (35) to Eqs. (26) and (27) shows that the non-normalized cpdf (34) is retrieved by replacing $N-(2p)^{-1}$ in the nonstandardized cpdf (26) by N, i.e., resulting in a marginal increase of the number of independent samples. In other words, the non-normalized cpdf is marginally closer to the asymptotic ensemble pdf ($N\rightarrow+\infty$) than the nonstandardized cpdf, resulting in slightly smaller uncertainties. This result is made plausible by the fact that the uncertainty of the sampling mean value is smaller than for the sampling standard deviation. It is worth emphasizing that, even though $f_U(u;N)$ is for the (dimensioned) energy density U, the chosen route for arriving at this pdf—i.e., whether via intermediary standardization or normalization in the cpdf of U—has an effect on the number of degrees of freedom of the end result but not on the functional form. In summary, whenever $2pN \gg 1$ (i.e.,

for most practical cases), standardization and normalization yield indistinguishable final results.

4. Intensity of biased field

As an extension of Eq. (22), the sampling cpdf of $U|S_U$ for the incoherently detected intensity of a biased field is a generalization of the so-called modified Nakagami-Rice m distribution, given for $p=1$ in self-sufficient form by
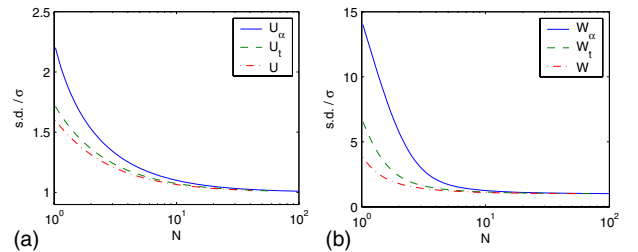

FIG. 5. (Color online) Sampling standard deviations (s.d.) as a function of N, standardized by corresponding ensemble standard deviations $\sigma = \sigma_{U_\alpha}$, σ_{U_t}, σ_U, (a) for Bessel K sampling distributions (26) of U_α, U_t, and U and (b) for Fisher-Snedecor F sampling distributions (29) of $W_\alpha = U_\alpha/S_{U_\alpha}$, $W_t = U_t/S_{U_t}$, and $W=U/S_U$.

$$f_{U_\alpha | S_{U_\alpha}}(u_\alpha | s_{U_\alpha}) = \frac{\sqrt{1 + 2k_{U_\alpha}}}{s_{U_\alpha}} \exp\left(-\sqrt{1 + 2k_{U_\alpha}} \frac{u_\alpha + u_{\alpha 0}}{s_{U_\alpha}}\right)$$

$$\times I_0\left(2\sqrt{1 + 2k_{U_\alpha}} \frac{\sqrt{u_{\alpha 0} u_\alpha}}{s_{U_\alpha}}\right), \quad (36)$$

with

$$k_{U_\alpha} \triangleq \frac{|E_{\alpha 0}|^2}{\langle |E_\alpha - E_{\alpha 0}|^2 \rangle} = \frac{1 - n_{U_\alpha}^2 + \sqrt{1 - n_{U_\alpha}^2}}{n_{U_\alpha}^2}, \quad (37)$$

where n_{U_α} is a sample value of $\nu_{U_\alpha} \triangleq \sigma_{U_\alpha}/\mu_{U_\alpha}$. Since $\sigma_{U_\alpha} = \sigma_{U_\alpha - u_{\alpha 0}}$ for any constant (deterministic) value $u_{\alpha 0}$, the pdf $f_{S_{U_\alpha}}(s_{U_\alpha}; N)$ is still given by Eq. (23) with $p=1$. Thus,

$$f_{U_\alpha}(u_\alpha; N) = \frac{C'_{U_\alpha}}{\sigma_{U_\alpha}} \int_0^{+\infty} \sqrt{1 + 2k_{U_\alpha}} \left(\frac{s_{U_\alpha}}{\sigma_{U_\alpha}}\right)^{N-5/2}$$

$$\times \exp\left[-\left(N - \frac{1}{2}\right)\frac{s_{U_\alpha}}{\sigma_{U_\alpha}}\right]$$

$$\times \exp\left(-\sqrt{1 + 2k_{U_\alpha}} \frac{u_\alpha + u_{\alpha 0}}{s_{U_\alpha}}\right)$$

$$\times I_0\left(2\sqrt{1 + 2k_{U_\alpha}} \frac{\sqrt{u_{\alpha 0} u_\alpha}}{s_{U_\alpha}}\right) ds_{U_\alpha}. \quad (38)$$

Note that k_{U_α} depends implicitly on s_{U_α}: to first approximation, $k_{U_\alpha} \simeq s_{U_\alpha}/\mu_{U_\alpha}$.

B. Coherent detection

In the case of estimating $f_U(u; N)$ from measurements of E, the sampling pdf takes a different form from that for incoherent detection, as we show next. Knowing the pdf of $E_\alpha = E'_\alpha - jE''_\alpha$, we can derive the pdf of $U = |E|^2 = p|E_\alpha|^2$, where $|E_\alpha|^2 \equiv E'^2_\alpha + E''^2_\alpha = U_\alpha$ is the intensity of a Cartesian field component and similarly for the electric or magnetic power $P \propto U$. Since $f_{U'^{(\prime)}_\alpha}(u'^{(\prime)}_\alpha) \propto f_{E'^{(\prime)}_\alpha}(e'^{(\prime)}_\alpha = \sqrt{u'^{(\prime)}_\alpha})/\sqrt{u'^{(\prime)}_\alpha}$, we obtain

$$f_{U_\alpha}(u_\alpha; N) = C_{U_\alpha} \int_0^{u_\alpha} f_{U'_\alpha}(x; N) f_{U''_\alpha}(u_\alpha - x; N) dx \quad (39)$$

$$= C_{U_\alpha} \int_0^{u_\alpha} \frac{f_{E'_\alpha}(\sqrt{x}; N) f_{E''_\alpha}(\sqrt{u_\alpha - x}; N)}{\sqrt{x}\sqrt{u_\alpha - x}} dx, \quad (40)$$

where C_{U_α} is a normalization constant. The general expression (40) makes allowance for the fact that E'_α and E''_α may, in principle, have different pdfs (functionally and/or parametrically), although in most cases the pdf of E_α is circular, i.e., $f_{E'_\alpha} = f_{E''_\alpha}$. The sample pdfs of $U_t \equiv U_x + U_y$ and $U \equiv U_x + U_y + U_z$ follow similarly from two- and threefold convolutions of Eq. (40), respectively. Figure 6 shows the pdf (40) for
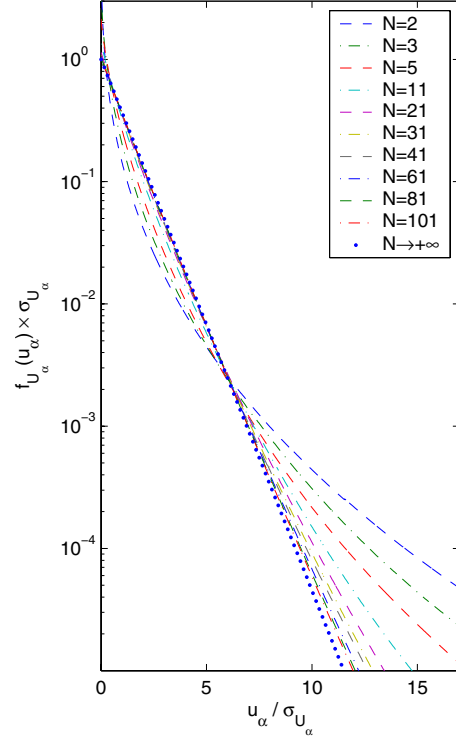

FIG. 6. (Color online) Probability density function of intensity or energy density of Cartesian component of field ($p=1$) derived from coherent detection at selected values of N: Bessel K sampling pdf of U_α [Eq. (40)]. The right tail becomes thinner for increasing values of N.

selected values of N. Comparing Fig. 6 to Fig. 2(a) shows that coherent detection yields a sampling pdf of U_α that exhibits an even larger kurtosis and heavier tail than for incoherent detection.

If U_α is to be compared to measured data, then the sampling pdf can be similarly calculated from $f_{X'_\alpha}$ and $f_{X''_\alpha}$ as

$$f_{W_\alpha}(w_\alpha) = C_{W_\alpha} \int_0^{w_\alpha} \frac{f_{X'_\alpha}(\sqrt{x}; N) f_{X''_\alpha}(\sqrt{w_\alpha - x}; N)}{\sqrt{x}\sqrt{w_\alpha - x}} dx, \quad (41)$$

where $W_\alpha \triangleq U_\alpha/S_{U_\alpha}$.

IV. FIELD AMPLITUDE

A. Incoherent detection

1. Nonstandardized field amplitude

The sampling pdf of $A \triangleq \sqrt{E'^2 + E''^2}$ follows in a manner similar to that for U. In this case, $A | S_A$ has a χ_{2p} cpdf, given in self-sufficient form as

$$f_{A|S_A}(a|s_A) = \frac{2\left[p - \left(\frac{\Gamma\left(p + \frac{1}{2}\right)}{\Gamma(p)}\right)^2\right]^p}{\Gamma(p)s_A}\left(\frac{a}{s_A}\right)^{2p-1}$$

$$\times \exp\left\{-\left[p - \left(\frac{\Gamma\left(p + \frac{1}{2}\right)}{\Gamma(p)}\right)^2\right]\left(\frac{a}{s_A}\right)^2\right\},$$

$$(42)$$

which has the Rayleigh distribution as a special case for $p = 1$, while S_A has the χ_{2pN-1} distribution

$$f_{S_A}(s_A;N) = \frac{2\left[pN - \frac{1}{2} - \left(\frac{\Gamma(pN)}{\Gamma\left(pN - \frac{1}{2}\right)}\right)^2\right]^{pN-1/2}}{\left(pN - \frac{1}{2}\right)\Gamma\left(pN - \frac{1}{2}\right)\sigma_{S_A}}\left(\frac{s_A}{\sigma_{S_A}}\right)^{2(pN-1)}$$

$$\times \exp\left\{-\left[pN - \frac{1}{2} - \left(\frac{\Gamma(pN)}{\Gamma\left(pN - \frac{1}{2}\right)}\right)^2\right]\left(\frac{s_A}{\sigma_{S_A}}\right)^2\right\},$$

$$(43)$$

with σ_{S_A} and σ_A related via

$$\sigma_{S_A} = \sigma_A \sqrt{1 - \frac{1}{pN - \frac{1}{2}}\left(\frac{\Gamma(pN)}{\Gamma\left(pN - \frac{1}{2}\right)}\right)^2}. \quad (44)$$

The sampling pdf of A is obtained as a marginal pdf of $f_{A,S_A}(a,s_A;N)$ and is again a Bessel K distribution, but of yet another type compared to Eqs. (13) and (26), viz.,

$$f_A(a;N)$$

$$= \int_0^{+\infty} f_{A|S_A}(a|s_A)f_{S_A}(s_A;N)ds_A$$

$$= \frac{C_A}{\sigma_A}\left(\frac{a}{\sigma_A}\right)^{p(N+1)-3/2}$$

$$\times K_{p(N-1)-1/2}\left(2\sqrt{\left[p - \left(\frac{\Gamma\left(p + \frac{1}{2}\right)}{\Gamma(p)}\right)^2\right]\left(pN - \frac{1}{2}\right)\frac{a}{\sigma_A}}\right),$$

$$(45)$$

where C_A is obtained, with the aid of [[25], Eq. (6.561.16)], as

$$C_A \triangleq \frac{4}{\Gamma(p)\Gamma\left(pN - \frac{1}{2}\right)}\left[p - \left(\frac{\Gamma\left(p + \frac{1}{2}\right)}{\Gamma(p)}\right)^2\right]^{[p(N+2)-1]/2}$$

$$\times \left(pN - \frac{1}{2}\right)^{[p(N+1)-1]/2}. \quad (46)$$

The pdf (45) for $p = 1$ has been obtained in [3] for the above-mentioned scenario of a random walk with fluctuating number of steps with negative binomial distribution. For general p, this pdf has been retrieved as a limit distribution for imperfect reverberation in [23].

The pdfs (45) for $p = 1$, 2, and 3 are shown in Figs. 7(a), 8(a), and 9(a), respectively, for selected values of N. Figure 10(a) shows the corresponding standardized standard deviations of Eq. (29). Compared to Fig. 5(a), the increase of the standard deviations with decreasing N is generally smaller and less dependent on dimensionality.

2. Standardized field amplitude

For comparison to the empirical pdf of a field amplitude measured by an electric or magnetic field probe, we consider the sampling pdf of the ratio of the variates A and S_A, viz.,

$$V \triangleq \frac{A}{S_A}. \quad (47)$$

The calculation of $f_V(v;N)$ is detailed in Sec. 3 of the Appendix, where the final result is shown to be

$$f_V(v;N) = C_V v^{2p-1}\left[1 + \frac{p - \left(\frac{\Gamma\left(p + \frac{1}{2}\right)}{\Gamma(p)}\right)^2}{pN - \frac{1}{2}}v^2\right]^{-[p(N+1)-1/2]},$$

$$(48)$$

with

$$C_V \triangleq \frac{2}{\left(pN - \frac{1}{2}\right)^p}\left[p - \left(\frac{\Gamma\left(p + \frac{1}{2}\right)}{\Gamma(p)}\right)^2\right]^p \frac{\Gamma\left(pN - \frac{1}{2} + p\right)}{\Gamma\left(pN - \frac{1}{2}\right)\Gamma(p)}. \quad (49)$$

The sampling pdf (48) can be referred to as a root-F distribution and constitutes a counterpart of Eqs. (19) and (29). Figure 10(b) shows its standardized standard deviation as a function of N for $p = 1$, $p = 2$, and $p = 3$. Compared to Fig. 5(a), an even sharper decrease with increasing N is observed in case of low dimensionality.

3. Amplitude of biased field

Unfortunately, unlike Eq. (36), the cpdf $f_{A_\alpha|S_{A_\alpha}}(a_\alpha|s_{A_\alpha})$ cannot be expressed in self-sufficient closed form because σ_{A_α} for the Nakagami-Rice cpdf of A depends in a compli-
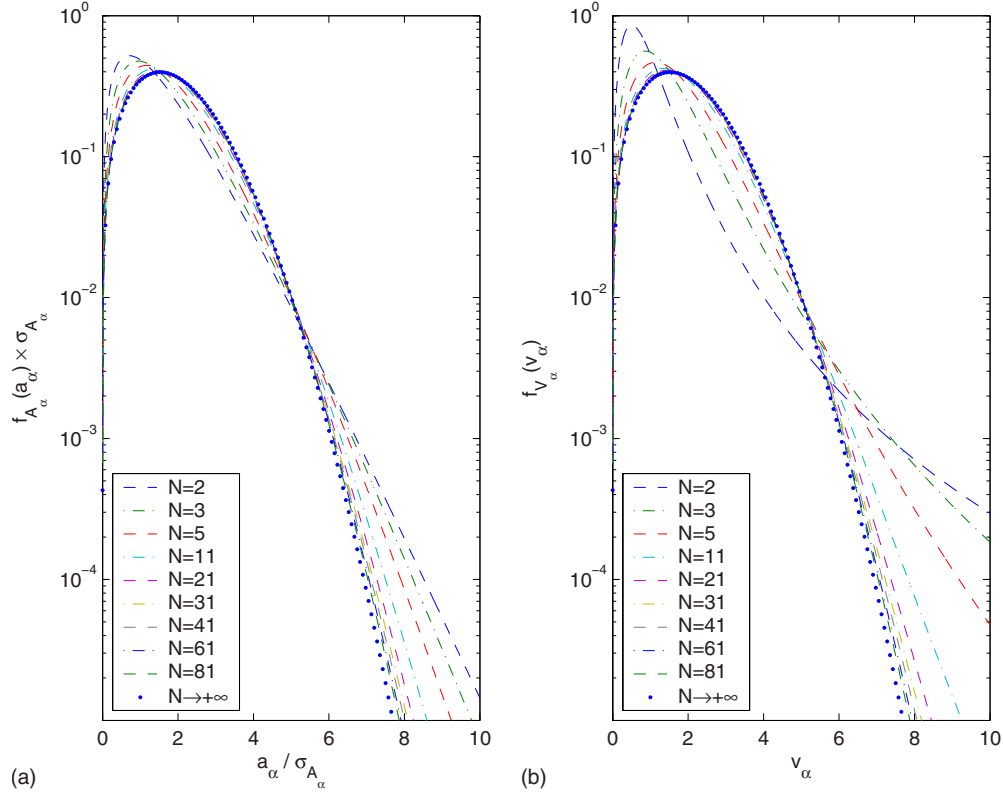
FIG. 7. (Color online) Sampling probability density function of amplitude of Cartesian component of field ($p=1$) at selected values of N based on incoherent detection. (a) Bessel K sampling pdf (45) for A_α. (b) Root-F pdf (48) for $V_\alpha = A_\alpha / S_{A_\alpha}$. In both plots, the right tail becomes thinner for increasing values of N.

cated manner on $\sigma_{E'^{(\prime)}}$. Therefore, we do not further pursue this case. A simpler approach is to derive $f_A(a;N)$ via variate transformation of Eq. (38).

B. Coherent detection

Using the variate transformation $A=\sqrt{U}$, the pdf of the local-field magnitude $A=\sqrt{A_x^2+A_y^2+A_z^2}\equiv|E|\propto\sqrt{U}$ follows. With $A_\alpha \triangleq \sqrt{E_\alpha'^2+E_\alpha''^2}$, Eq. (40) yields

$$f_{A_\alpha}(a_\alpha;N) = a_\alpha f_{U_\alpha}(u_\alpha = a_\alpha^2)$$
$$= C_{A_\alpha} a_\alpha \int_0^{a_\alpha^2} \frac{f_{E_\alpha'}(\sqrt{x};N) f_{E_\alpha''}(\sqrt{a_\alpha^2 - x};N)}{\sqrt{x}\sqrt{a_\alpha^2 - x}} dx, \quad (50)$$

where C_{A_α} is a normalization constant. The pdf for A_α is shown for selected values of N in Fig. 11 and for A in Fig. 12.

In fact, one may consider the amplitude of the sampling field itself as a marginal of the joint sampling pdf $f_{E',E''}(e',e'';N)$, followed by variate transformation to the amplitude $A=\sqrt{E'^2+E''^2}$ and phase $\Phi=\tan^{-1}(E''/E')$. Assuming that E' and E'' are statistically independent (which, strictly, requires them to be normally distributed) so that $f_{E',E''}(e',e'';N)=f_{E'}(e';N)f_{E''}(e'';N)$, then

$$f_A(a;N) = \frac{C_A}{\sigma_A} a^{pN-1} \int_{-\pi}^{\pi} (|\cos\phi - (a_0/a)||\sin\phi|)^{pN/2-1}$$
$$\times K_{pN/2-1}\left(\sqrt{pN-1}\frac{|a\cos\phi - a_0|}{\sigma_{E'}}\right)$$
$$\times K_{pN/2-1}\left(\sqrt{pN-1}\frac{|a\sin\phi|}{\sigma_{E''}}\right) d\phi, \quad (51)$$

where $a_0 \triangleq \mu_{E'}$, with $\mu_{E''}=0$.

V. EXTENSION TO NON-GAUSSIAN ENSEMBLE DISTRIBUTIONS OF THE FIELD: ITERATIVE BAYESIAN SCHEME

From the theorem of total probability, it follows that

$$f_{S_{E'^{(\prime)}}|E'^{(\prime)}} \propto f_{E'^{(\prime)}|S_{E'^{(\prime)}}} f_{S_{E'^{(\prime)}}}. \quad (52)$$

For non-Gaussian $E'^{(\prime)}$, for which the prior pdf $f_{S_{E'^{(\prime)}}}$ is more difficult to determine than in the exposition given before, Eq. (52) can be used in an iterative process by means of an update equation for $f_{S_{E'^{(\prime)}}}$, where the latter can be assigned an initial χ_{N-1} distribution $f_{S_{E'^{(\prime)}}}^{(0)}$. This prior distribution, together with the non-Gaussian $f_{E'^{(\prime)}|S_{E'^{(\prime)}}}$, then allows for calculating the posterior $f_{S_{E'^{(\prime)}}|E'^{(\prime)}}$ that serves as the "prior" pdf for the next iteration. Explicitly, denoting the ith iteration in
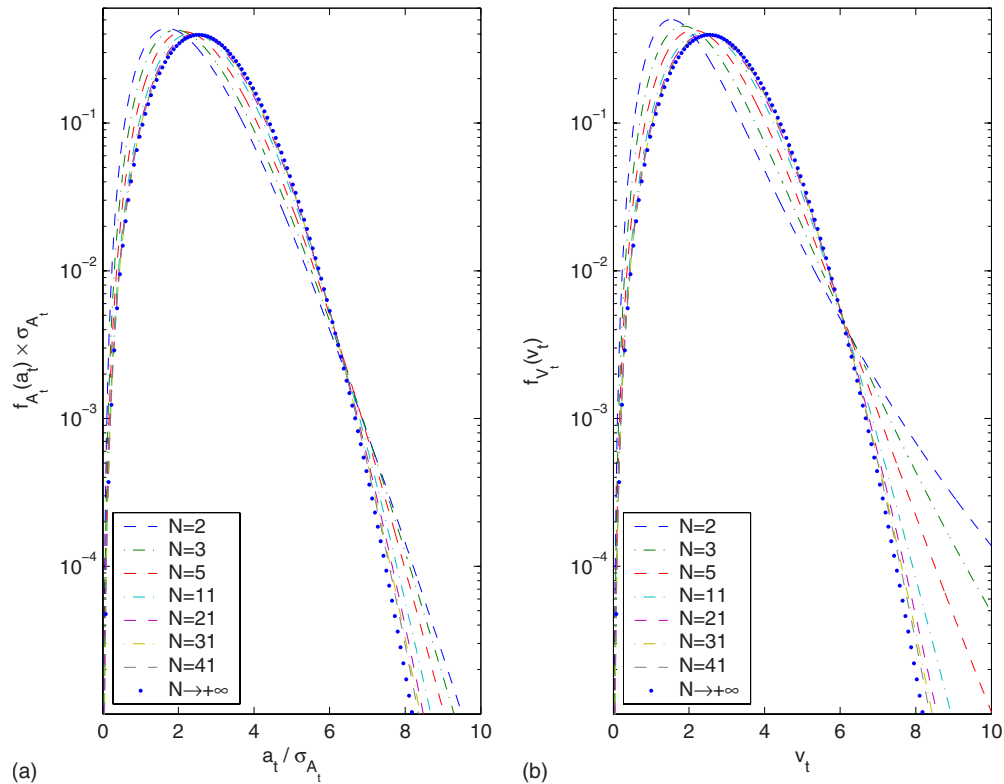
FIG. 8. (Color online) Sampling probability density function of amplitude of planar field ($p=2$) at selected values of N based on incoherent detection. (a) Bessel K pdf (45) for A_t. (b) Root-F pdf (48) for $V_t = A_t/S_{A_t}$. In both plots, the right tail becomes thinner for increasing values of N.

this scheme by the superscript "(i)," the iteration process is specified by

$$f_{S_{E'(\prime)}}^{(i+1)} = f_{S_{E'(\prime)}|E'(\prime)}^{(i)} \qquad (53)$$

for $i = 0, 1, \ldots$, thus yielding $f_{E'(\prime)|S_{E'(\prime)}}^{(n)}$ after n iterations, with similar relations for the intensity and amplitude.

In general, Eqs. (52) and (53) can be used even with empirical pdfs $f_{E'(\prime)|S_{E'(\prime)}}$. A similar equation and procedure can be used for determining the intensity or magnitude for incoherent detection. This outline of a procedure is sketched here for sake of completeness and guidance. However, no explicit results are included because they require knowledge of $f_{E'(\prime)|S_{E'(\prime)}}$ which must follow from a separate investigation, e.g., from experiment. Further study is needed with respect to the demonstration of convergence of Eq. (53) to a stable pdf.

VI. CONFIDENCE INTERVALS

95% confidence interval boundaries from sampling pdfs of E, U, A as well as X, W, V and their components are compared to corresponding boundaries for the ensemble pdfs in Figs. 13, 14, and 15, respectively. The figures show that $N \sim 10$ or larger is needed in order for the sampling confidence interval boundaries to be close to the ensemble boundaries. For example, for an overmoded Fabry-Pérot resonator, a resonator length of the order of 5 wavelengths or larger is needed to achieve this (cf. Sec. II A 1).

VII. CONCLUSION

In this paper, we studied sampling distributions for the analytic complex-valued field, the intensity (energy density, power), and the magnitude for Gaussian statistically homogeneous random electromagnetic waves. The main results are Eqs. (13)–(15), (17), (19), (26), (29), (45), and (48). A common feature is that lowering the number of degrees of freedom characterizing sampling distributions results in their tails becoming heavier and in a consequent associated increase of widths of confidence intervals compared to the Gauss normal, χ_{2p}^2 and χ_{2p} ensemble distributions, respectively. Accurate knowledge of the tail behavior is also critically important in the estimation of the distribution of the maximum value [22,30]. Furthermore, it was shown that standardized quantities (i.e., the sampled random field, magnitude or intensity divided by its own sample standard deviation, whereby the latter is itself considered as a random variable whose sample value is calculated from the sample data set itself) exhibit sampling pdfs that are characterized by a wider spread than for the case where that quantity has an *a priori* known (ensemble) standard deviation. The reason is that in the former case, the ratio of random variables defines a bivariate sampling distribution whose (univariate) marginal pdf is sought, whereas in the latter case, the sampling pdf is univariate from the outset. The differences in sampling distributions arising from choosing normalization rather than standardization were shown to be negligible in all practical cases.
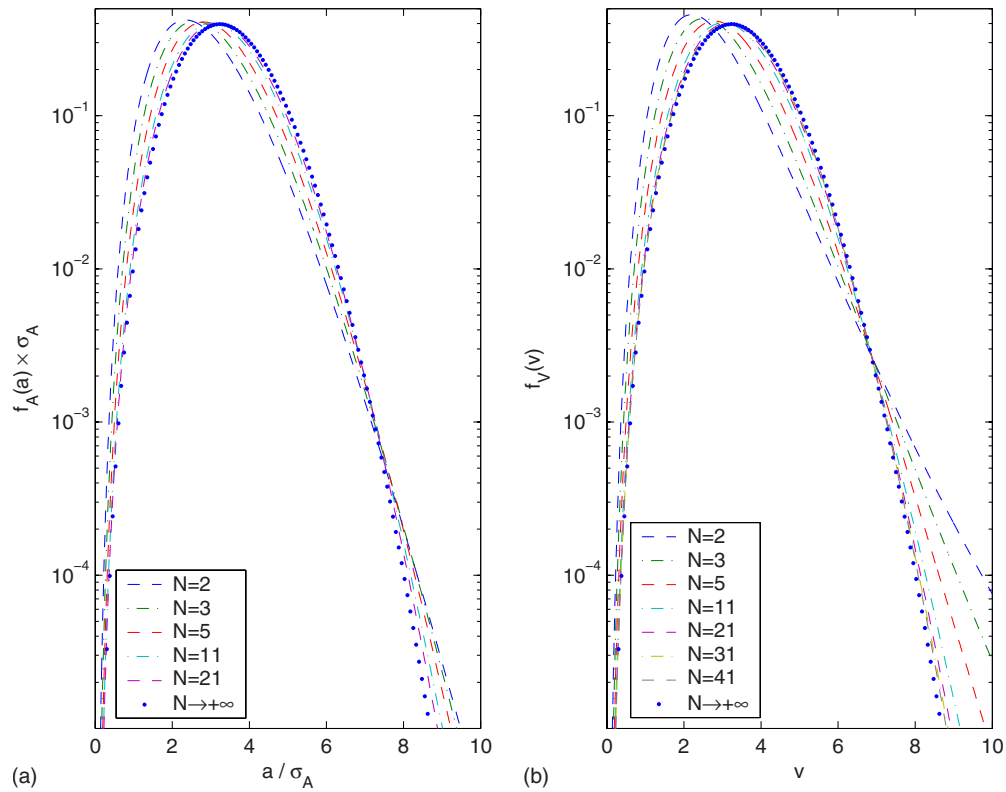
FIG. 9. (Color online) Sampling probability density function of amplitude of total (vector) field ($p=3$) at selected values of N based on incoherent detection. (a) Bessel K pdf (45) for A. (b) Root-F pdf (48) for $V=A/S_A$. In both plots, the right tail becomes thinner for increasing values of N.

While the focus in this paper was on the simplest of *a priori* chosen conditional pdfs for the local instantaneous field in unbounded media, extension to some more general cases and boundary-value problems is straightforward. For example, compound exponential distributions for anisotropic ideal random fields near a conducting or dielectric boundary [9,33] can be used instead, leading to the total (vectorial) intensity and amplitude of 3D random fields near a planar isotropic surface by simple superposition. Finally, note that the present analysis was concerned with purely local fields (point-wise characterization), while non-Gaussianity is known to arise also as a result of nonlocality (i.e., spatial or temporal averaging) of fields [22,34].
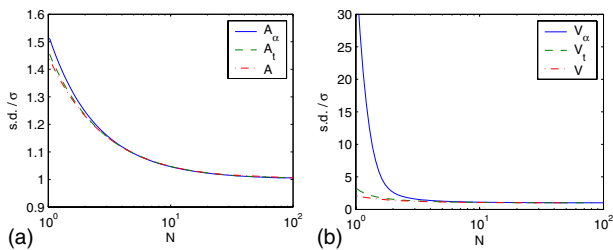

FIG. 10. (Color online) Sampling standard deviations (s.d.) as a function of N, standardized by corresponding ensemble standard deviations $\sigma = \sigma_{A_\alpha}$, σ_{A_t}, σ_A, (a) for Bessel K sampling distributions (45) of A_α, A_t, and A and (b) for root-F sampling distributions (48) of $V_\alpha = A_\alpha/S_{A_\alpha}$, $V_t = A_t/S_{A_t}$, and $V = A/S_A$.
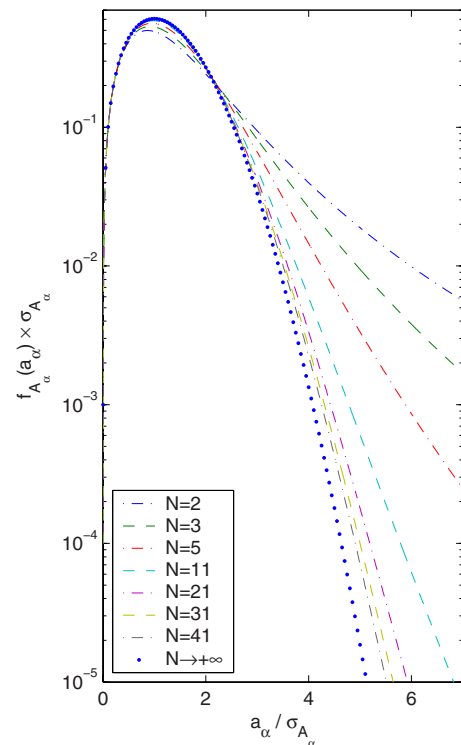

FIG. 11. (Color online) Sampling probability density function of magnitude of Cartesian component of field ($p=1$) at selected values of N, derived for coherent detection. The right tail becomes thinner for increasing values of N.
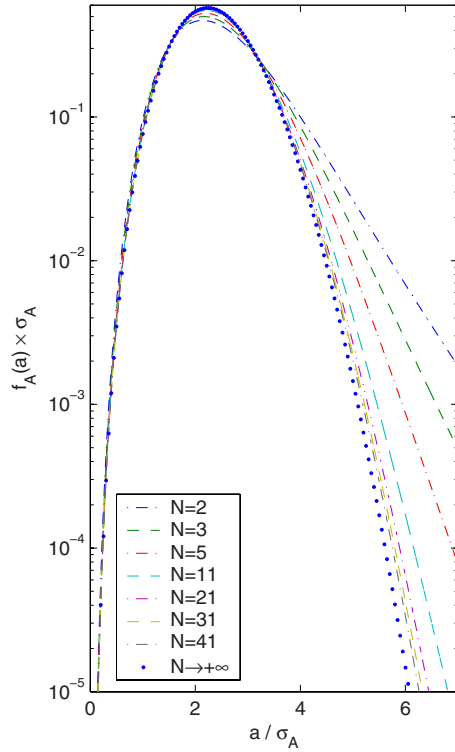
FIG. 12. (Color online) Sampling probability density function of magnitude of total (vector) field ($p=3$) at selected values of N, derived for coherent detection. The right tail becomes thinner for increasing values of N.
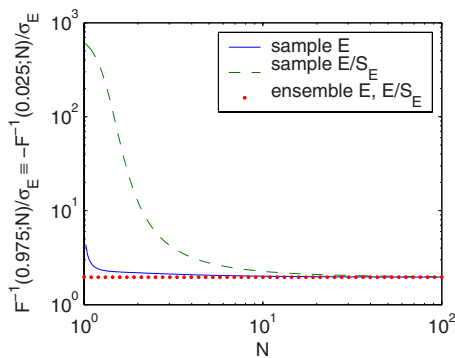
FIG. 13. (Color online) Upper boundaries of 95% confidence intervals for real or imaginary parts of E_α, E_t, or E. The lower quantile $F^{-1}(0.025) \equiv -F^{-1}(0.975)$ is located symmetrically with respect to $e=0$.
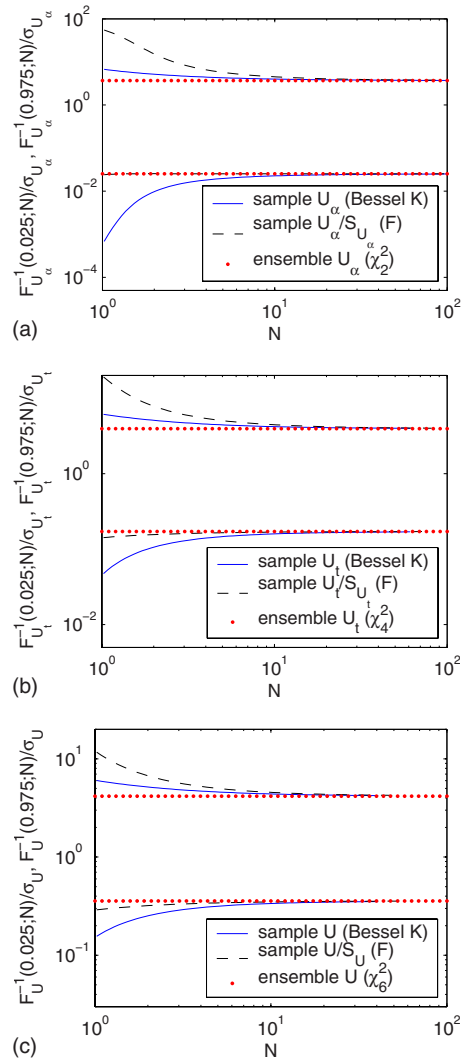

FIG. 14. (Color online) Lower and upper boundaries of 95% confidence intervals (a) for a 1D Cartesian component U_α ($p=1$), (b) for a 2D planar component U_t ($p=2$), and (c) for the 3D vectorial U ($p=3$), normalized by the respective sampling standard deviations. For each line type, the lower and upper curves represent 2.5% and 97.5% percentiles, respectively.

APPENDIX: SAMPLING DISTRIBUTIONS OF SAMPLE-STANDARDIZED FIELD, INTENSITY, AND AMPLITUDE

1. Field

Here, we derive the one-dimensional sample-standardized sampling distribution for the intensity $|E|^2$ or energy density $U \propto |E|^2$ of a random statistically homogeneous Cartesian or vector electric (or, by extension, magnetic) field E. The pdf of an ideal random field E is circular with independent and identically distributed (i.i.d.) real (in-phase) and imaginary (quadrature) components $E' \triangleq \mathrm{Re}(E)$ and $E'' \triangleq \mathrm{Im}(E)$. As a result, these components can be studied in isolation from each other. The parent (ensemble) distribution of E is a central Gauss normal distribution ($\langle E \rangle = 0$). Therefore, the standardized N-point sample variance $D_{N-1} \triangleq (N-1)S^2_{E'^{(\prime)}}/\sigma^2_{E'^{(\prime)}} = \Sigma^N_{i=1}(E'^{(\prime)}_i - M_{E'^{(\prime)}})^2/\sigma^2_{E'^{(\prime)}}$ exhibits a χ^2_{N-1} pdf, while

$D_1 \triangleq (E'^{(\prime)} - M_{E'^{(\prime)}})^2/\sigma^2_{E'^{(\prime)}}$ has a χ^2_1 pdf. Consequently, the ratio

$$X'^{(\prime)} \triangleq \frac{E'^{(\prime)} - M_{E'^{(\prime)}}}{S_{E'^{(\prime)}}} = \sqrt{\frac{D_1}{D_{N-1}/(N-1)}} \qquad (A1)$$

has a Student t sampling distribution with $N-1$ degrees of freedom, whence for $E'^{(\prime)}$ itself,

$$f_{E'^{(\prime)}}(e'^{(\prime)};N) = \frac{\Gamma\left(\dfrac{N}{2}\right)}{\sqrt{\pi}\Gamma\left(\dfrac{N-1}{2}\right)\sqrt{N-1}\,s_{E'^{(\prime)}}}$$
$$\times \left[1 + \frac{1}{N-1}\left(\frac{e'^{(\prime)} - m_{E'^{(\prime)}}}{s_{E'^{(\prime)}}}\right)^2\right]^{-N/2} \tag{A2}$$

for $N > 1$, where $e'^{(\prime)}$, $m_{E'^{(\prime)}}$, and $s_{E'^{(\prime)}}$ are sample values. Compared to the sample value $s_{E'^{(\prime)}}$ for the parent pdf, the sampling pdf Eq. (A2) exhibits an increased sampling standard deviation, viz., $\sqrt{(N-1)/(N-3)}\,s_{E'^{(\prime)}}$ for $N > 3$.

Typically, the Student t distribution arises in the characterization of the sample *mean*, i.e., for $[(M_{E'^{(\prime)}} - \langle E'^{(\prime)}\rangle)/(\sigma_{E'^{(\prime)}}/\sqrt{N})]/(S_{E'^{(\prime)}}/\sigma_{E'^{(\prime)}})$, instead of $[(E'^{(\prime)} - M_{E'^{(\prime)}})/\sigma_{E'^{(\prime)}}]/(S_{E'^{(\prime)}}/\sigma_{E'^{(\prime)}})$ as in Eq. (A1). Without lack of generality, we further use the simplified definition $X'^{(\prime)} \triangleq E'^{(\prime)}/S_{E'^{(\prime)}}$, i.e., $M_{E'^{(\prime)}}=0$, because each sample set can always be centralized by its own sample mean value while maintaining its sampling pdf. In this case Eq. (A2) reduces to Eq. (19).

2. Field intensity

The square of $X'^{(\prime)}$, represented as $Y'^{(\prime)}/S_{Y'^{(\prime)}} \triangleq X'^{(\prime)2} = E'^{(\prime)2}/S^2_{E'^{(\prime)}}$, exhibits a t^2 sampling distribution that follows from Eq. (A2) as

$$f_{Y'^{(\prime)}}(y'^{(\prime)};N) = \frac{\Gamma\left(\dfrac{N}{2}\right)}{2\sqrt{\pi}\Gamma\left(\dfrac{N-1}{2}\right)\sqrt{N-1}}$$
$$\times \left[\frac{y'^{(\prime)}}{s_{Y'^{(\prime)}}}\left(1 + \frac{y'^{(\prime)}}{(N-1)s_{Y'^{(\prime)}}}\right)^N\right]^{-1/2}, \tag{A3}$$

which is a Fisher-Snedecor $F_{1,N-1}$ pdf of the ratio of the standard χ^2_1 variate D_1 and the standard χ^2_{N-1} variate D_{N-1} (both being statistically independent because $M_{E'^{(\prime)}}$ and $S_{E'^{(\prime)}}$ are independent for Gauss normal $E'^{(\prime)}$), whereby each variate is divided by its corresponding number of degrees of freedom, i.e.,

$$t^2 = F_{1,N-1} = \frac{\chi^2_1/1}{\chi^2_{N-1}/(N-1)}. \tag{A4}$$

To find the sampling distribution of a squared Cartesian or vectorial EM field with $2p$ i.i.d. components $Y'^{(\prime)}_i$ (corre-
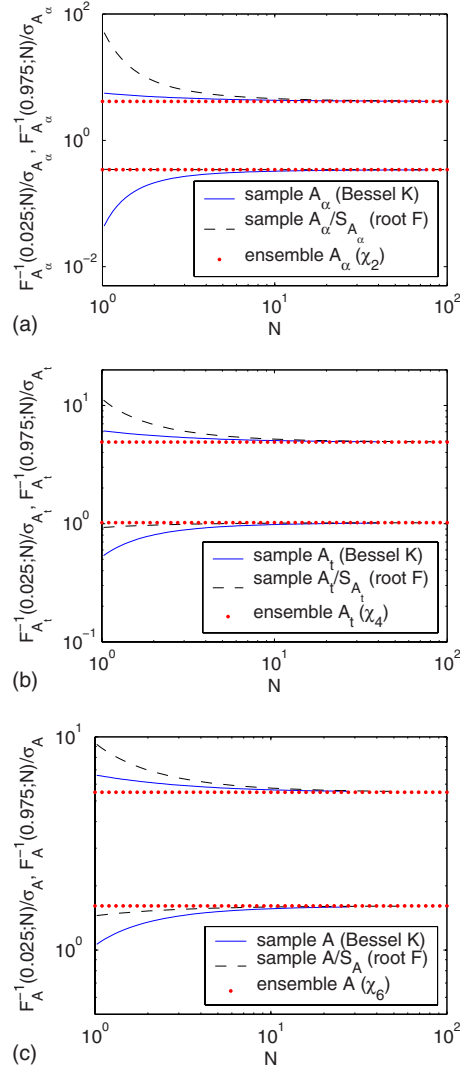

FIG. 15. (Color online) Lower and upper boundaries of 95% confidence intervals (a) for a 1D Cartesian component A_α ($p=1$), (b) for a 2D planar component A_t ($p=2$), and (c) for the 3D vectorial A ($p=3$), normalized by the respective sampling standard deviations. For each line type, the lower and upper curves represent 2.5% and 97.5% percentiles, respectively.

sponding to a p-dimensional analytic complex-valued field), i.e., $\sigma_{Y'^{(\prime)}_i} = \sigma^2_X$, we consider the ratio Z/D_Z, where

$$Z \triangleq \frac{Y' + Y''}{\sigma_{Y'^{(\prime)}}} = \sum_{i=1}^{p}\left(\frac{Y'_i}{\sigma_{Y'}} + \frac{Y''_i}{\sigma_{Y''}}\right) = \sum_{i=1}^{2p}\frac{(X_i - m_X)^2}{\sigma^2_X} \tag{A5}$$

has a standard χ^2_{2p} distribution, on account of the addition theorem for $2p$ i.i.d. standard χ^2_1 variates, and

$$D_Z \triangleq \frac{(2pN-1)S^2_{X'^{(\prime)}}}{\sigma^2_{X'^{(\prime)}}} \tag{A6}$$

exhibits a standard χ^2_{2pN-1} distribution, with $S^2_{X'^{(\prime)}} = \Sigma_{i=1}^{2pN}(X'^{(\prime)}_i - M_{X'^{(\prime)}})^2/(2pN-1)$. Hence, their ratio G is a scaled Fisher-Snedecor F variate with $(2p, 2pN-1)$ degrees of freedom

$$G \triangleq \frac{Z}{D_Z} \equiv \frac{2p}{2pN-1} \frac{Z/(2p)}{D_Z/(2pN-1)} = \frac{2p}{2pN-1} F_{2p,2pN-1}.$$

(A7)

With $\sigma_{|E|^2} = 2\sqrt{p}\sigma_{E'^{(\prime)}}^2$, the ratio Z/D_Z can be related to the standardized power or field intensity as

$$\frac{U}{S_U} = \frac{\sum\limits_{i=1}^{2p} E_i'^2}{2\sqrt{p}S_{E'}^2} = \frac{2pN-1}{2\sqrt{p}} \frac{\sum\limits_{i=1}^{2p}(E_i'/\sigma_{E'})^2}{(2pN-1)S_{E'}^2/\sigma_{E'}^2} = \frac{2pN-1}{2\sqrt{p}} \frac{Z}{D_Z}.$$

(A8)

Thus, combining Eqs. (A7) and (A8) yields

$$W \triangleq \frac{U}{S_U} = \sqrt{p} F_{2p,2pN-1}.$$

(A9)

With Eq. (A7), upon scaling the standard $F_{2p,2pN-1}$ distribution, the sampling pdf of G is

$$f_G(g;N) = \frac{\Gamma\left(pN - \frac{1}{2} + p\right)}{\Gamma\left(pN - \frac{1}{2}\right)\Gamma(p)} \frac{g^{p-1}}{(1+g)^{pN-1/2+p}}.$$

(A10)

For the squared Cartesian in-phase field component $[\mathrm{Re}(E)]^2$ or the squared quadrature component $[\mathrm{Im}(E)]^2$ (i.e., for $p = 1/2$), Eq. (A10) reduces to Eq. (A3) as expected. Finally, from Eq. (A9), the sampling distribution of W follows as

$$f_W(w;N)$$
$$= \frac{\Gamma\left(pN - \frac{1}{2} + p\right)}{\Gamma\left(pN - \frac{1}{2}\right)\Gamma(p)} \frac{p^{p/2}}{\left(pN - \frac{1}{2}\right)^p} \frac{w^{p-1}}{\left(1 + \frac{\sqrt{p}}{pN - \frac{1}{2}}w\right)^{pN-1/2+p}}.$$

(A11)

This represents the pdf of the standardized received sampled power W at w, i.e., for the ratio of sampled values u and s_U.

In the limit $N \to +\infty$, the exponent $p(N+1) - \frac{1}{2}$ in Eq. (A11) reduces to $pN - \frac{1}{2}$, the prefactor $\Gamma(pN - \frac{1}{2} + p)/\Gamma(pN - \frac{1}{2}) = (pN - \frac{1}{2}) \cdots (pN - \frac{3}{2} + p)$ for $p \geq 1$ becomes $(pN - \frac{1}{2})^p$, and s_U approaches the ensemble statistic σ_U, whence

$$f_W(w;N) \to f_U(u) = \frac{p^{p/2}}{\Gamma(p)\sigma_U}\left(\frac{u}{\sigma_U}\right)^{p-1}\exp\left(-\sqrt{p}\frac{u}{\sigma_U}\right),$$

(A12)

which is the ensemble χ_{2p}^2 limit pdf, as expected. The result agrees with a well-known limit theorem from probability theory [7] stating that $F_{m,n}(x)$ converges to $\chi_m^2(mx)$ when

$n/m \to +\infty$, whence, $F_q(m,n) \to \chi_q^2(m)/m$ for the corresponding quantiles. In the limit $N \to +\infty$, the asymptotic mean value of W is

$$\langle W \rangle = \frac{2pN-1}{2pN-3}\sqrt{p} \to \sqrt{p}$$

(A13)

and the standard deviation valid for $pN > 5/2$ is

$$\sigma_W = \sqrt{\frac{2(2pN-1)^2(2pN+2p-3)}{2p(2pN-3)^2(2pN-5)}}p \to 1. \quad \text{(A14)}$$

Thus, we find that the coefficient of variation, i.e.,

$$\frac{\sigma_W}{\langle W \rangle} = \sqrt{\frac{2pN+2p-3}{p(2pN-5)}} \to \frac{1}{\sqrt{p}},$$

(A15)

has its value reduced to that for the χ_{2p}^2 ensemble distribution when $N \to +\infty$, whereas for small N, its value is substantially larger, indicating larger relative uncertainty.

3. Field amplitude

For the standardized field magnitude $V \triangleq A/S_A = \sqrt{(S_V^2/S_W)W}$, with

$$\frac{\sigma_Z^2}{\sigma_W} = \frac{\sigma_A^2}{\sigma_{A^2}} = \frac{p - \left(\dfrac{\Gamma\left(p + \frac{1}{2}\right)}{\Gamma(p)}\right)^2}{\sqrt{p}}$$

(A16)

valid for $\chi_{2p}^{(2)}$ distributions, from variate transformation of Eq. (A11) and noting that

$$\frac{w}{s_W} = \left(\frac{v}{s_V}\right)^2 = \frac{v^2}{s_W}\frac{s_W}{s_V^2}, \quad dw = 2v\frac{s_W}{s_V^2}dv, \quad \text{(A17)}$$

we obtain the sampling pdf of V at $v = a/s_A$ as

$$f_V(v;N) = C_V\, v^{2p-1}\left[1 + \frac{p - \left(\dfrac{\Gamma\left(p + \frac{1}{2}\right)}{\Gamma(p)}\right)^2}{pN - \frac{1}{2}}v^2\right]^{-(pN+p-1/2)},$$

(A18)

which can be referred to as a root-F distribution, where

$$C_V \triangleq \frac{2}{\left(pN - \frac{1}{2}\right)^p}\left[p - \left(\frac{\Gamma\left(p + \frac{1}{2}\right)}{\Gamma(p)}\right)^2\right]^p \frac{\Gamma\left(pN - \frac{1}{2} + p\right)}{\Gamma\left(pN - \frac{1}{2}\right)\Gamma(p)}.$$

(A19)

[1] D. W. Schaefer and P. N. Pusey, Phys. Rev. Lett. **29**, 843 (1972).

[2] E. Jakeman and P. N. Pusey, IEEE Trans. Antennas Propag. **24**, 806 (1976).

[3] E. Jakeman, J. Phys. A **13**, 31 (1980).

[4] S. Primak, J. LoVetri, and J. Roy, IEEE Trans. Electromagn. Compat. **44**, 266 (2002).

[5] E. Kogan and M. Kaveh, Phys. Rev. B **52**, R3813 (1995).

[6] A. A. Chabanov and A. Z. Genack, Phys. Rev. E **72**, 055602(R) (2005).

[7] H. Cramér, *Mathematical Methods of Statistics* (Princeton University Press, Princeton, 1946), Chap. 27, p. 29.

[8] J. G. Kostas and B. Boverie, IEEE Trans. Electromagn. Compat. **33**, 366 (1991).

[9] L. R. Arnaut, Radio Sci. **42**, RS3001 (2007).

[10] G. E. Becker and S. H. Autler, Phys. Rev. **70**, 300 (1946).

[11] S. Deus, P. M. Koch, and L. Sirko, Phys. Rev. E **52**, 1146 (1995).

[12] J. de Rosny, Ph. Roux, M. Fink, and J. H. Page, Phys. Rev. Lett. **90**, 094302 (2003).

[13] M. Kamionkowski, A. Kosowsky, and A. Stebbins, Phys. Rev. D **55**, 7368 (1997).

[14] R. Khatri and B. D. Wandelt, Phys. Rev. D **79**, 023501 (2009).

[15] C. Räth, G. E. Morfill, G. Rossmanith, A. J. Banday, and K. M. Górski, Phys. Rev. Lett. **102**, 131301 (2009).

[16] W. Martienssen and E. Spiller, Am. J. Phys. **32**, 919 (1964).

[17] G. Maret and P. E. Wolf, Z. Phys. B: Condens. Matter **65**, 409 (1987).

[18] P. Zakharov, F. Cardinaux, and F. Scheffold, Phys. Rev. E **73**, 011413 (2006).

[19] B. Daino, G. de Marchis, and S. Piazolla, Electron. Lett. **15**, 755 (1979).

[20] G. C. Papen and P. M. Murphy, J. Lightwave Technol. **17**, 817 (1999).

[21] J. Pearce, Z. Jian, and D. M. Mittleman, Opt. Lett. **30**, 2843 (2005).

[22] L. R. Arnaut, IEEE Trans. Electromagn. Compat. **43**, 305 (2001).

[23] L. R. Arnaut, IEEE Trans. Electromagn. Compat. **45**, 357 (2003).

[24] P. Beckmann, *Probability in Communication Engineering* (Harcourt, Brace & World, New York, 1967).

[25] I. S. Gradstheyn and I. M. Ryzhik, *Table of Integrals, Series, and Products*, 7th ed. (Academic, New York, 2007).

[26] A. T. McKay, Biometrika **24**, 39 (1932).

[27] F. McNolty, Sankhya, Ser. B **B29**, 235 (1967).

[28] M. Nakagami, in *Statistical Methods in Radio Wave Propagation*, edited by W. C. Hoffman (Pergamon, London, 1960), pp. 3–36.

[29] B. D. Carter and M. D. Springer, SIAM J. Appl. Math. **33**, 542 (1977).

[30] L. R. Arnaut, NPL Report TQE 2, edition 2.0, pp. 1–136, Dec. 2008 http://publications.npl.co.uk/npl_web/pdf/TQE2.pdf.

[31] "Student" W. S. Gosset, Biometrika **6**, 1 (1908).

[32] L. R. Arnaut and D. A. Knight, Phys. Rev. Lett. **98**, 053903 (2007).

[33] L. R. Arnaut, IEEE Trans. Electromagn. Compat. **48**, 359 (2006).

[34] S. Jung and H. L. Swinney, Phys. Rev. E **72**, 026304 (2005).